

A Phenomenological Study of Bottom Quark Fragmentation in Top Quark Decay at Hadron Colliders

G. Corcella^{1,2,3} and F. Mescia⁴

¹*Museo Storico della Fisica e Centro Studi e Ricerche E. Fermi,
Piazza del Viminale 1, I-00185 Roma, Italy*

²*Scuola Normale Superiore, Piazza dei Cavalieri 7, I-56126, Pisa, Italy*

³*INFN, Sezione di Pisa, Largo Fibonacci 3, I-56127, Pisa, Italy*

⁴*Universitat de Barcelona,
Departamento d'Estructura i Constituents de la Materia (ECM)
and Institut de Ciències del Cosmos (ICC),
Av. Diagonal 647, E-08028, Barcelona, Spain*

Abstract

Top-quark physics is one of the main fields of investigation at the Tevatron accelerator and, ultimately, at the LHC. We perform a phenomenological analysis of $t\bar{t}$ events at hadron colliders, with a focus on observables relying on bottom-quark fragmentation in top-quark decay. In particular, we investigate the B -lepton invariant-mass distribution in the dilepton channel and give an estimate of the contribution of bottom fragmentation to the Monte Carlo uncertainty on the top-quark mass reconstruction.

1 Introduction

Bottom-quark fragmentation in top decay ($t \rightarrow bW$) is one of the main sources of uncertainty in the measurements of the top-quark properties, such as its mass. In fact, b -quark fragmentation enters in the uncertainty on the b -energy scale, contributing to the Monte Carlo systematics on the top-mass reconstruction (see, e.g., the top quark analyses from CDF [1, 2] and D0 [3] at the Tevatron accelerator).

Monte Carlo generators, such as the general-purpose HERWIG [4] and PYTHIA [5] codes, implementing hard-scattering processes, parton showers, hadronization and underlying event, are widely used to simulate $t\bar{t}$ events at hadron colliders. In particular, HERWIG and PYTHIA simulate the hadronization transition according to the cluster [6] and string [7] models¹, respectively, containing a few parameters which need to be tuned to data, e.g., from LEP or SLD experiments.

In order to estimate the contribution of bottom fragmentation to the Monte Carlo systematic error on top-quark observables, one typically compares the results yielded by the two codes and varies the hadronization parameters describing the $b \rightarrow B$ transition within suitable ranges. At the LHC, it is worthwhile mentioning the study [10], where it was proposed that one could reconstruct the top-quark mass in the dilepton channel, by using the decays $B \rightarrow J/\psi$ and $J/\psi \rightarrow \mu^+\mu^-$, B being a b -flavoured hadron. The top mass was then fitted from the peak value of the $m_{J/\psi\ell}$ or $m_{\mu\ell}$ invariant-mass spectra, ℓ being a charged lepton in W decay $W \rightarrow \ell\nu$. This analysis estimates that, in the phase of luminosity 10^5 pb^{-1} , after setting suitable cuts on transverse momenta and rapidities of final-state leptons, one can reconstruct the top mass with an error $\Delta m_t \simeq 1 \text{ GeV}$. The contribution of b -fragmentation to Δm_t is found to be about 600 MeV and is estimated by using the PYTHIA generator along with the Peterson fragmentation function², varying the ϵ parameter in the range $(5.0 \pm 0.5) \times 10^{-3}$. At the Tevatron, the recent CDF analysis [2] identifies jets containing a candidate muon from semileptonic B -decays (so-called ‘soft muon b -tagging’) and measures the top mass by using the invariant mass $m_{\ell\mu}$, with ℓ still coming from W -boson decay. The overall Monte Carlo uncertainty, due to the modelling of $t\bar{t}$ production and decay in HERWIG and PYTHIA, including b -fragmentation as well³, was estimated to be $\Delta m_t \simeq 2.1 \text{ GeV}$ [2].

From the point of view of Monte Carlo generators, however, the default parametriza-

¹As an option, PYTHIA allows one to interface its showers to fragmentation functions, such as the Bowler [8] or Peterson [9] models

²The Peterson fragmentation function reads: $D(x, \epsilon) = A/[x(1 - 1/x - \epsilon/(1 - x))]$, where x is the hadron energy fraction, A a normalization constant and ϵ a parameter to be tuned to experimental data.

³The uncertainties due to the treatment of initial- and final-state radiation were, however, calculated separately from the Monte Carlo systematic error.

tions of both HERWIG and PYTHIA are unable to fit LEP and SLD data on B -hadron production at the Z^0 pole [11]. In Ref. [11] the cluster and string models were tuned to such data: after the fits, PYTHIA managed to describe the B -energy spectrum very well, whereas HERWIG was only marginally consistent.

Following [11], in this paper we wish to perform a phenomenological study of $t\bar{t}$ events at hadron colliders, taking particular care about observables relying on b -quark fragmentation in top decay, and investigate possible discrepancies between HERWIG and PYTHIA, which may affect the Monte Carlo systematic error on the top-mass reconstruction. In particular, our investigation will be especially useful for the top mass extractions according to Refs. [2, 10], as those methods strongly depend on the Monte Carlo simulation of the $b \rightarrow B$ transition in top decay.

In Section 2 we shall briefly review the results of Ref. [11] on fitting cluster and string models to LEP and SLD B -production data. In Section 3 we shall present a few results for observables in $t\bar{t}$ events depending on the description of b -quark fragmentation. In Section 4, as an example of application of our analysis, we shall try to estimate the uncertainty on the extraction of m_t in the dilepton channel from a fit of the invariant mass $m_{B\ell}$ distribution, ℓ being a lepton from W decay. In Section 5 we shall summarize the main results of our study and make some concluding remarks.

2 Fitting hadronization models to LEP and SLD B -production data

In this section we shall shortly summarize the main findings of Ref. [11], where the cluster and string models, which simulate hadronization in HERWIG and PYTHIA, were fitted to LEP and SLD data on the B -hadron spectrum. Ref. [11] considered data on b -flavoured hadron production from the LEP experiments ALEPH [12] and OPAL [13], and from SLD [14]. In particular, the ALEPH sample was made of B -mesons, whereas OPAL and SLD also had a small fraction of B -baryons, such as the Λ_b . The B spectrum in $e^+e^- \rightarrow b\bar{b}$ annihilation at the Z^0 pole was studied in terms of the quantity

$$x_B = \frac{2p_B \cdot p_Z}{m_Z^2}. \quad (1)$$

In Eq. (1), p_B and p_Z are the B and Z^0 four-momenta, respectively. In Z^0 rest frame, $x_B = 2E_B/m_Z$, the normalized B -energy fraction. As for PYTHIA, it was chosen the scenario with parton showers ordered in virtuality, with an option to reject non-angular-ordered emissions. Angular ordering is correctly satisfied by the HERWIG cascades [15].

HERWIG	PYTHIA
CLSMR(1) = 0.4 (0.0)	
CLSMR(2) = 0.3 (0.0)	PARJ(41) = 0.85 (0.30)
DECWT = 0.7 (1.0)	PARJ(42) = 1.03 (0.58)
CLPOW = 2.1 (2.0)	PARJ(46) = 0.85 (1.00)
PSPLT(2) = 0.33 (1.00)	
$\chi^2/\text{dof} = 222.4/61$ (739.4/61)	$\chi^2/\text{dof} = 45.7/61$ (467.9/61)

Table 1: Best-fit hadronization parameters in HERWIG and PYTHIA, after comparing with the B -hadron energy spectrum measured at OPAL, ALEPH and SLD, along with the χ^2 per degree of freedom. In brackets, we quote the default values of such parameters.

The default parametrizations of HERWIG and PYTHIA ⁴ were unable to acceptably reproduce such data, yielding $\chi^2/\text{dof} = 793.4/61$ and $467.9/61$, respectively. In [11], the two event generators were therefore fitted to the x_B spectra: the choice of the authors was to tune only parameters associated with hadronization and leave unchanged the ones related to hard scattering and parton showers. As pointed out in [11], whenever one fits just one measured quantity, such as x_B , the risk is that one may spoil the comparison with other observables, e.g., light-flavour fragmentation. Therefore, the fits performed in [11] are not an official tuning of HERWIG and PYTHIA, but just an attempt to understand whether the description of heavy-flavour fragmentation could be improved.

Table 1 summarizes the results of such fits: the χ^2 per degree of freedom refers to all data points, as if they were coming from one single experiment. In HERWIG, one fitted CLSMR(1) and CLSMR(2), namely the Gaussian smearing of the hadron direction with respect to the parent quark, PSPLT(2), a parameter ruling the mass spectrum of b -flavoured cluster decays, CLPOW, controlling the yield and meson/baryon production, and DECWT, determining the decuplet/octet ratio. As for PYTHIA, the three fitted parameters, namely PARJ(41), PARJ(42) and PARJ(46), are the a , b and r quantities in the Lund/Bowler fragmentation function [5, 8]:

$$f_B(z) \propto \frac{1}{z^{1+brm_b^2}} (1-z)^a \exp(-bm_T^2/z), \quad (2)$$

m_b and m_T being the b -quark mass and the B -hadron transverse mass respectively. From Table 1, we learn that, after the fit, PYTHIA reproduces pretty well the data, while HERWIG is only marginally consistent with the x_B spectra, although its description of

⁴ Ref. [11] used HERWIG 6.506 and PYTHIA 6.220. The latest fortran versions do not actually present any new features which may change the conclusions of Ref. [11].

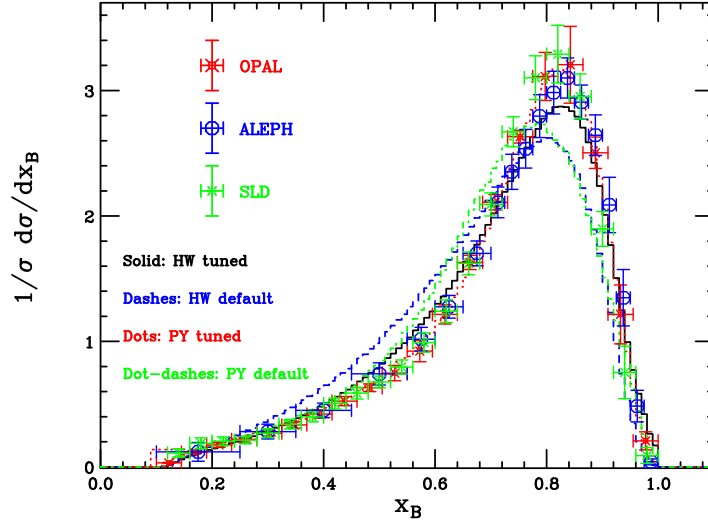


Figure 1: Data from LEP experiments on the B -hadron spectrum in e^+e^- annihilation, along with HERWIG and PYTHIA, according to their default versions and with the hadronization models tuned to such data.

the data is much better with respect to the default parametrization. The comparison between data, default and tuned HERWIG and PYTHIA is presented in Fig. 1. We note that PYTHIA, after the tuning, gives an excellent description of the data throughout all x_B -range, while the HERWIG prediction, even after fitting the cluster model, is still below the data around the peak and above the data for middle values of x_B . The problems exhibited by HERWIG when its predictions are compared with the x_B distributions, have been mostly fixed in the object-oriented version HERWIG++ [17], which implements an improved cluster model. In fact, Ref. [18] showed that it is enough tuning the shower cutoff to obtain a rather good fit of the SLD data. Although the employment of HERWIG++ and of the corresponding PYTHIA 8 code [19], written in C++, should be recommended, and not only for the better description of B -hadronization, the fortran versions of these generators are still widely used. In particular, fortran HERWIG provides the MC@NLO code [20], which implements the hard-scattering process at next-to-leading order (NLO), with parton showers and hadronization. Moreover, the so-called matrix-element generators, such as, for example, the ALPGEN [21] or MadGraph [22] programs, often employed to study backgrounds to $t\bar{t}$ events, are interfaced to fortran versions of HERWIG and PYTHIA for showers and hadronization. It is therefore still useful trying to improve the b -fragmentation sector in the fortran generators and compare their results for a few observables relevant to top-quark decay. The best fits presented in Table 1 will be the starting point for the phenomenological analysis which we shall carry out for $t\bar{t}$ events at hadron colliders.

Before closing this section, we point out that heavy-quark energy distributions can

also be obtained by using resummed calculations, such as Ref. [23] for e^+e^- annihilation, Ref. [24] for top decays and Ref. [25] for $H \rightarrow b\bar{b}$, H being the Standard Model Higgs boson. Such computations, based on the perturbative-fragmentation formalism [26], resum soft/collinear logarithms with an accuracy which is usually higher than parton-shower algorithms: therefore, comparisons with resummations, as done in [11], are useful to validate Monte Carlo generators and understand the role played by subleading logarithms. However, resummed computations are too inclusive to allow a complete investigation of final states. Also, they still need to be supplemented by phenomenological non-perturbative fragmentation functions, such as the models [8, 9, 27], to be comparable with experimental data on hadron production. In the following, we shall not only investigate the B -hadron energy fraction, but also observables for which resummed calculations are not currently available. Monte Carlo generators, giving an exclusive description of final states, are thus the best available tool to carry out our study.

3 Top-quark decay observables at hadron colliders

Given the HERWIG and PYTHIA best fits presented in the above Section, and relying on the universality of the hadronization transition, we wish to make predictions for top-decay observables depending on b -quark fragmentation, taking particular care about quantities which might be useful for Tevatron or LHC phenomenology.

3.1 B -hadron energy fraction in top decay

Let us consider top quark decay:

$$t(p_t) \rightarrow b(p_b)W(p_W)X(p_X), \quad (3)$$

where X stands for extra parton radiation, and the subsequent transition $b(p_b) \rightarrow B(p_B)$. A straightforward extension of the x_B variable in Eq. (1) is the following quantity:

$$x_B = \frac{1}{1 - m_W^2/m_t^2 + m_b^2/m_t^2} \frac{2p_B \cdot p_t}{m_t^2}. \quad (4)$$

x_B is a Lorentz-invariant variable which corresponds to the normalized B -energy fraction in top rest frame. At LEP and SLD, since the e^+e^- collision takes place at the Z^0 pole, the laboratory coincides with the Z^0 rest frame. On the contrary, at the Tevatron or LHC, the laboratory frame is not the top-quark rest frame, and therefore, in order to measure the x_B quantity, one would need all four components of top and B momenta. Such a measurement is obviously not straightforward; however, it is still interesting

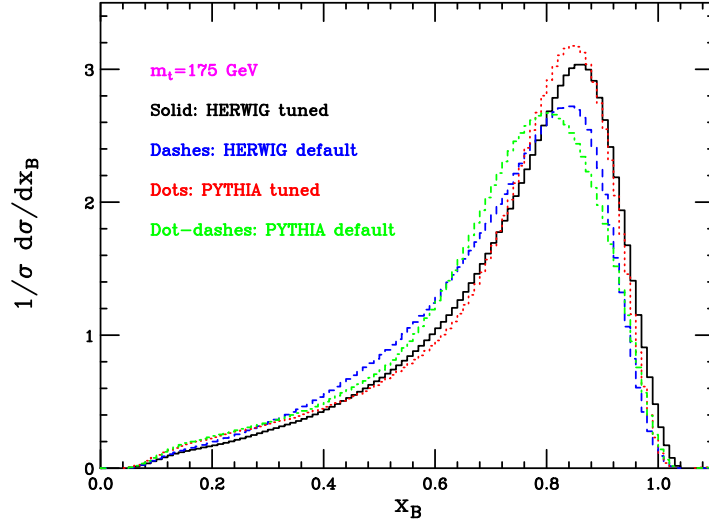


Figure 2: B -hadron spectrum in top decay, for $m_t = 175$ GeV, according to HERWIG and PYTHIA, using the default parametrizations and after fitting cluster and string models to LEP and SLD data.

presenting the x_B spectrum in top decay, in such a way to compare HERWIG and PYTHIA before and after the fits to e^+e^- data and understand how much x_B depends on the top quark mass. We point out that, as already observed in [11, 24], neglecting the top width, which is a reasonable approximation as long as experimental analyses set cuts of order 10 GeV or higher on the energy of final-state jets [28], the x_B spectrum is roughly independent of the production process. Therefore, in such an approximation, our results will be valid for both Tevatron and LHC: unless stated differently, the actual plots which will shall present are anyway obtained running HERWIG and PYTHIA in the LHC environment, i.e. pp collisions at $\sqrt{s} = 14$ TeV.

Fig. 2 exhibits the B -energy distribution in top decay yielded by PYTHIA and HERWIG, for $m_t = 175$ GeV, using default and tuned parametrizations. As in the e^+e^- case, the shapes of the spectra are remarkably modified once we fit string and cluster models: after the tuning, the distributions are somewhat narrower and shifted towards higher values of x_B . The comparison of the two tuned codes is similar to what observed in Fig. 1: HERWIG yields a broader distribution and is above PYTHIA for very large and middle values of x_B , whereas it is below PYTHIA around the peak and at small x_B . In Fig. 3 we present the same spectra, but varying the top mass from 171 to 179 GeV, and learn that x_B exhibits negligible dependence on the top mass, independently of the hadronization model which one uses. This is an interesting result: if one were able to measure x_B , it would be an ideal quantity to fit b -fragmentation parameters, with almost no dependence on the top-quark mass. However, as said above, for the time being, x_B in top decays is a hard observable to be accessed experimentally.

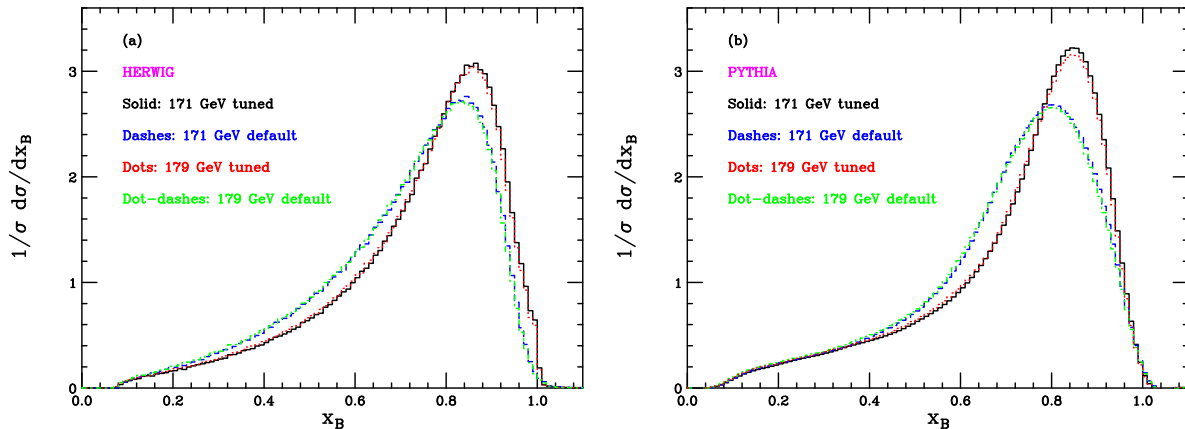


Figure 3: x_B spectrum in top decay for $m_t = 171$ and 179 GeV, according to default and tuned HERWIG (a) and PYTHIA (b).

3.2 B -lepton invariant-mass distribution in the dilepton channel

In this subsection, we investigate the B -lepton invariant mass ($m_{B\ell}$) distribution in the dilepton channel, where B is a b -flavoured hadron coming from top decay and ℓ a charged lepton in W decay ($W \rightarrow \ell\nu$). In fact, such a quantity is closely related to invariant masses $m_{\mu\ell}$ and $m_{J/\psi\ell}$, where the J/ψ 's and μ 's come from B decays, used in Refs. [2, 10], to fit the top mass at Tevatron and LHC, respectively.

The $m_{B\ell}$ invariant mass is another boost-invariant observable, just relying on top decay and not depending on the top-production phase. Such a quantity was already studied in Refs. [29, 30], in order to investigate the impact of matrix-element corrections to simulations of top decays in HERWIG. Ref. [30] also checked that the $m_{B\ell}$ distribution is roughly the same at the Tevatron and at the LHC, thus confirming that it is indeed independent of the production mechanism, which is mainly $q\bar{q} \rightarrow t\bar{t}$ at the Tevatron and $gg \rightarrow t\bar{t}$ at the LHC.

As done in the previous subsection for the x_B quantity, we first compare HERWIG and PYTHIA for a given value of m_t and then we vary the top mass. Fig. 4 presents the default and tuned $m_{B\ell}$ spectra for $m_t = 175$ GeV: in both codes, the fit to e^+e^- data has the effect to shift the distributions towards larger invariant-mass values⁵. As for the comparison between HERWIG and PYTHIA, the shapes of the curves yielded

⁵The results in Figs. 4 and 5 look different from the spectra presented in [29, 30], which were obtained using an unofficial preliminary HERWIG version, wherein a few bugs were lately found. The effect of matrix-element corrections to the HERWIG simulation of top decays found in [29, 30] is nevertheless still confirmed, when using the latest versions, with the bugs fixed.

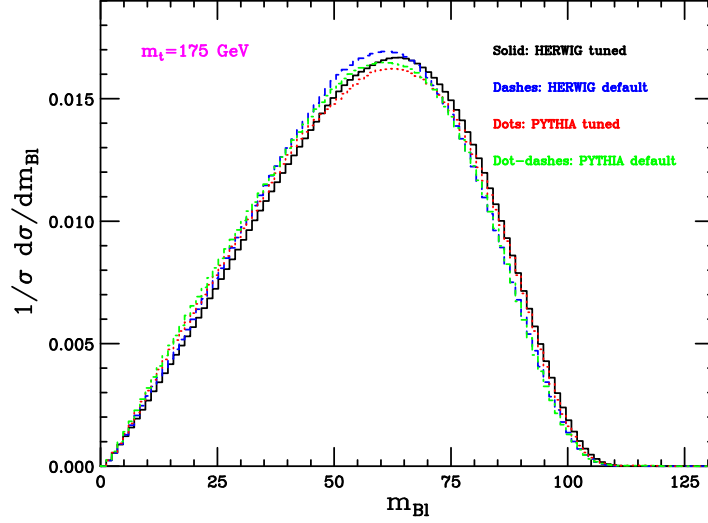


Figure 4: B -lepton invariant mass distribution, in top decay and in the dilepton channel, according to tuned and default HERWIG and PYTHIA, for $m_t = 175$ GeV.

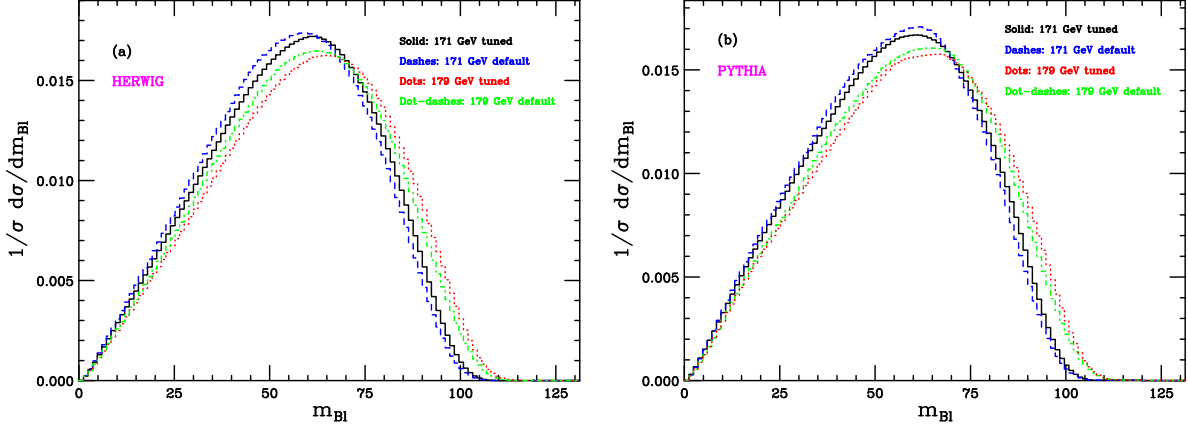


Figure 5: $m_{B\ell}$ spectrum in top decay for $m_t = 171$ and 179 GeV, according to default and tuned HERWIG (a) and PYTHIA (b).

by the two generators exhibit visible differences: HERWIG is above PYTHIA around the peak and below at small $m_{B\ell}$. At large $m_{B\ell}$ the discrepancy becomes very little, with HERWIG still giving a slightly higher differential cross section.

Looking at Fig. 5, we learn that the behaviours of HERWIG and PYTHIA spectra with respect to m_t are rather similar, in both default and tuned versions. Increasing m_t shifts the $m_{B\ell}$ spectrum towards higher invariant masses, as one would expect on physical grounds. We can anticipate that in Section 4 we shall thoroughly study the above spectra: we shall compute the Mellin moments and discuss of a possible extraction

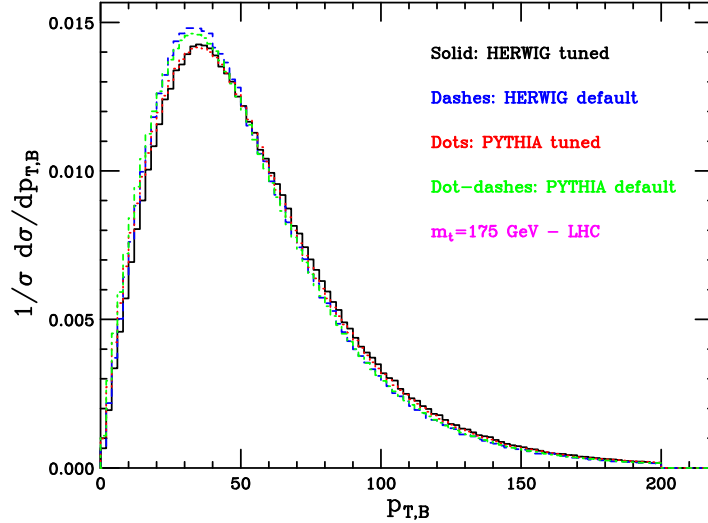


Figure 6: Transverse momentum distributions of B -hadrons in top decay at the LHC, according to tuned and default HERWIG and PYTHIA, for $m_t = 175$ GeV. $p_{T,B}$ is evaluated in the laboratory frame.

of the top mass from a fit of the mean value $\langle m_{B\ell} \rangle$.

3.3 B -hadron transverse momentum spectrum

In this subsection, we investigate the transverse momentum of the B -hadron in top decay ($p_{T,B}$) in the laboratory frame. Clearly, such an observable is not Lorentz invariant and, unlike x_B and $m_{B\ell}$, it does not depend only on the decay, but the production phase is essential in determining its spectrum. However, it is still useful to study such a quantity: a measurement of $p_{T,B}$ is more feasible than x_B and, as it happens, e.g., for the W/Z transverse momentum in Drell–Yan processes, can be useful to study the experimental acceptance for top events [32]. In the $p_{T,B}$ spectrum, the hadronization parameters will certainly play a role, although, as explained above, a number of other quantities, in particular initial-state radiation, are expected to be quite relevant.

In Fig. 6 we present the comparison between HERWIG and PYTHIA, default and tuned, for $m_t = 175$ GeV at the LHC; in Fig. 7 we plot the $p_{T,B}$ distribution for $m_t = 171$ and 179 GeV. As far as this observable is concerned, the discrepancy between HERWIG and PYTHIA looks smaller than for x_B and $m_{B\ell}$, with PYTHIA being slightly above HERWIG at small $p_{T,B}$ and below for middle-large transverse momenta. The effect of the tuning to LEP and SLD data is similar for both generators: less events at small x_B and at the peak, but a higher differential cross section for $p_{T,B} > 60$ GeV. To be more quantitative, the average value of $p_{T,B}$ for $m_t = 175$ GeV reads $\langle p_{T,B} \rangle \simeq 50.66$ and 50.59

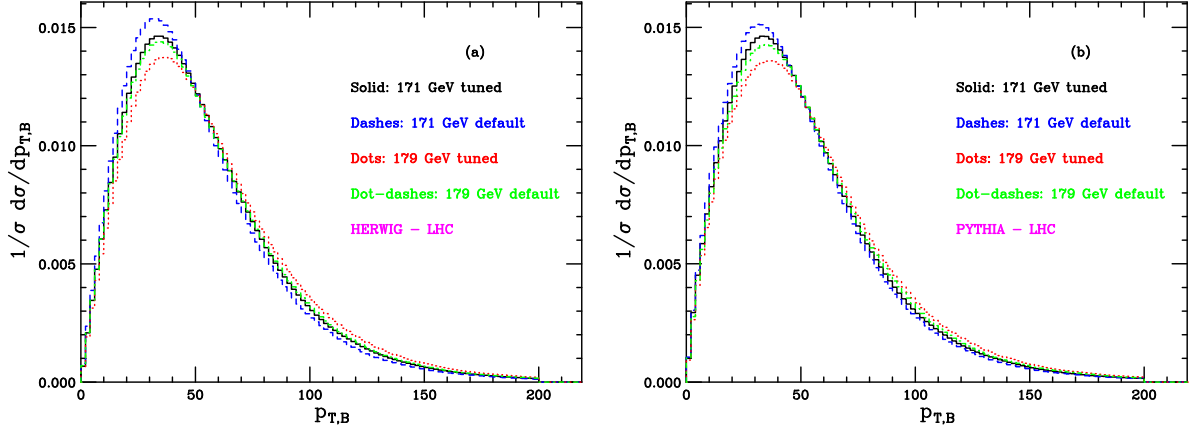


Figure 7: $p_{T,B}$ spectrum for $m_t = 171$ and 179 GeV, according to default and tuned HERWIG (a) and PYTHIA (b), at the LHC

GeV, for default HERWIG and PYTHIA respectively. After tuning cluster and string models, HERWIG yields $\langle p_{T,B} \rangle \simeq 53.01$ GeV, whereas PYTHIA $\langle p_{T,B} \rangle \simeq 52.20$ GeV. As for the top-mass dependence of this observable, a higher m_t results in less events around the peak value, and more with a large transverse-momentum b -flavoured hadron.

Since we observed that $p_{T,B}$ is not Lorentz-invariant and depends on the $t\bar{t}$ production mechanism, it is interesting investigating such a quantity even at the Tevatron accelerator, i.e. $p\bar{p}$ collisions at 1.96 GeV, where the production mechanism is mostly $q\bar{q} \rightarrow t\bar{t}$, whereas gluon-gluon fusion dominates at the LHC. In Fig. 8 we present the B transverse-momentum distribution at the Tevatron, for $m_t = 175$ GeV, given by default and tuned HERWIG and PYTHIA. We learn that at Tevatron energies the effect of the fits is qualitatively similar to what found at the LHC: less events are simulated at small transverse momentum and about the peak, while there are more top-decay B -hadrons at large $p_{T,B}$. The mean values are $\langle p_{T,B} \rangle \simeq 47.91$ and 47.66 GeV, according to default HERWIG and PYTHIA, whereas, when using the parametrization in Table 1, HERWIG gives $\langle p_{T,B} \rangle \simeq 50.23$ and PYTHIA 49.02 GeV. Hence, at both Tevatron and LHC, the two codes give more similar results when using the default parametrizations, while the discrepancy gets larger after the tuning.

In Fig. 9 we use instead the two codes with the fragmentation parameters tuned to LEP and SLD data: in Fig. 9 (a) we show the $p_{T,B}$ spectrum for $m_t = 171$ and 179 GeV, while, for the sake of comparison, in Fig. 9 (b) we present HERWIG and PYTHIA predictions at the Tevatron and at the LHC, using $m_t = 175$ GeV. The dependence of the $p_{T,B}$ spectrum on the top mass is like the one observed at LHC: a higher m_t shifts the B transverse-momentum distribution towards larger $p_{T,B}$. As for the comparison Tevatron/LHC, it shows indeed that we are dealing with an observables depending on the $t\bar{t}$ production stage and on the boost from the laboratory frame to the top rest frame,

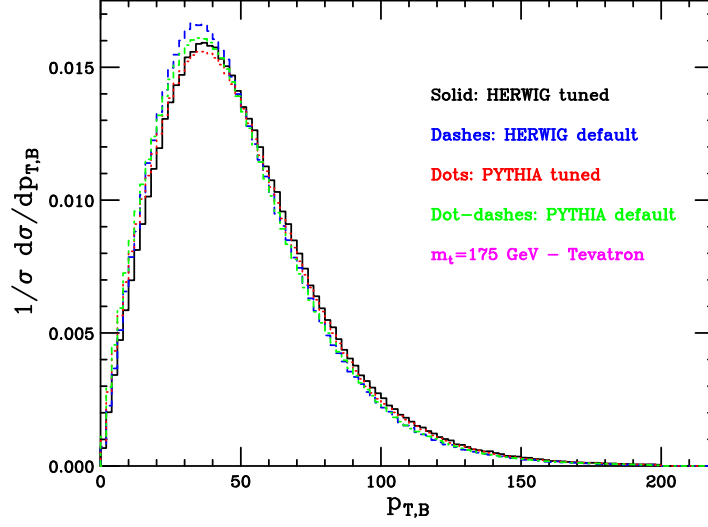


Figure 8: As in Fig. 6, but at the Tevatron accelerator.

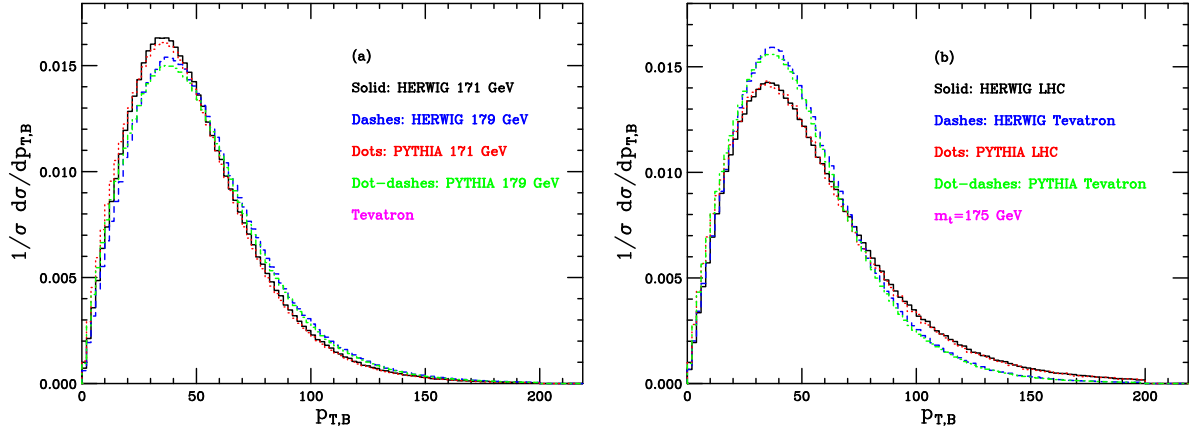


Figure 9: (a): $p_{T,B}$ spectrum for $m_t = 171$ and 179 GeV, according to tuned versions of HERWIG and PYTHIA at the Tevatron. (b): Comparison of LHC and Tevatron B -hadron transverse momentum spectra, given by tuned HERWIG and PYTHIA, for $m_t = 175$ GeV.

where top decay is performed. At the Tevatron, due to the lower available energy, most events are simulated for $p_{T,B} < 70$ GeV; at the LHC, the large- $p_{T,B}$ tail is instead more relevant with respect to the Tevatron.

4 Extracting the top mass from the $m_{B\ell}$ spectrum

As the B -lepton invariant mass is a Lorentz-invariant quantity, depending only on top decay and visibly sensitive to the top mass (see Fig. 5), we can think of using $m_{B\ell}$ to fit m_t . Also, after convoluting $m_{B\ell}$ with the $B \rightarrow J/\psi$ or $B \rightarrow \mu$ spectra, one will obtain the $m_{J/\psi\ell}$ and $m_{\mu\ell}$ distributions, employed in Refs. [2, 10] to extract m_t at the LHC and at the Tevatron, respectively.

Ideally, if we had data on $m_{B\ell}$, we may directly use them to validate the Monte Carlo tools and fit the cluster/string models. For the time being, we try to express the $m_{B\ell}$ spectra in terms of the top mass by computing the first few Mellin moments in the range $171 \text{ GeV} < m_t < 179 \text{ GeV}$. After observing that the fits to LEP and SLD do have a strong impact on top-decay observables depending on b -fragmentation, hereafter we shall stick to the best-fit parametrizations quoted in Table 1.

m_t (GeV)	$\langle m_{B\ell} \rangle$ (GeV)	$\langle m_{B\ell}^2 \rangle$ (GeV ²)	$\langle m_{B\ell}^3 \rangle$ (GeV ³)	$\langle m_{B\ell}^4 \rangle$ (GeV ⁴)
171	55.23	3.49×10^3	2.39×10^5	1.74×10^8
173	56.12	3.60×10^3	2.51×10^5	1.85×10^8
175	56.95	3.71×10^3	2.62×10^5	1.96×10^8
177	57.86	3.82×10^3	2.74×10^5	2.08×10^8
179	58.68	3.93×10^3	2.86×10^5	2.20×10^8

Table 2: First four moments of the $m_{B\ell}$ spectrum in top decay, yielded by HERWIG, after tuning the cluster model to ALEPH, OPAL and SLD data, for $171 \text{ GeV} < m_t < 179 \text{ GeV}$.

m_t (GeV)	$\langle m_{B\ell} \rangle$ (GeV)	$\langle m_{B\ell}^2 \rangle$ (GeV ²)	$\langle m_{B\ell}^3 \rangle$ (GeV ³)	$\langle m_{B\ell}^4 \rangle$ (GeV ⁴)
171	54.38	3.41×10^3	2.33×10^5	1.69×10^8
173	55.23	3.51×10^3	2.43×10^5	1.79×10^8
175	56.08	3.62×10^3	2.55×10^5	1.90×10^8
177	56.89	3.72×10^3	2.66×10^5	2.01×10^8
179	57.76	3.84×10^3	2.78×10^5	2.13×10^8

Table 3: As in Table 2, but using the PYTHIA event generator.

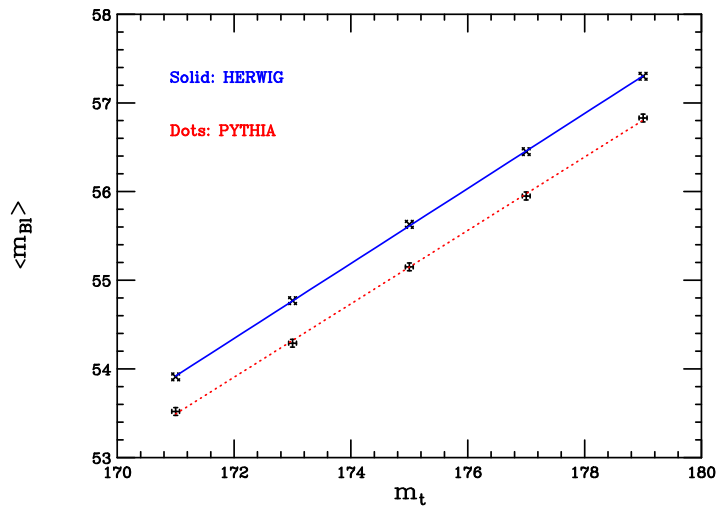


Figure 10: Linear fits of $\langle m_{B\ell} \rangle$ as a function of m_t , as obtained from HERWIG and PYTHIA codes.

We present the first four moments yielded by HERWIG and PYTHIA in Tables 2 and 3, respectively ⁶. From the comparison, we learn that HERWIG systematically yields moments which are larger than PYTHIA, as was already predictable looking at Fig. 4. Furthermore, according to both codes, the moments of the $m_{B\ell}$ spectrum linearly increase with respect to the top mass.

In order to give an estimate of the Monte Carlo uncertainty due to modelling b -quark fragmentation, we perform a linear fit of the average value $\langle m_{B\ell} \rangle$ in terms of m_t , by means of the least-square method ⁷. The linear fit works very well and the best fits are the following:

$$\langle m_{B\ell} \rangle \simeq -18.41 \text{ GeV} + 0.42 m_t, \quad \delta = 0.013 \text{ GeV} \quad (\text{HERWIG}), \quad (5)$$

$$\langle m_{B\ell} \rangle \simeq -17.30 \text{ GeV} + 0.41 m_t, \quad \delta = 0.032 \text{ GeV} \quad (\text{PYTHIA}), \quad (6)$$

where δ is the mean square deviation in the fit. The best-fit straight lines, as a function of m_t , are plotted in Fig. 10: we see that, for a given measurement of $\langle m_{B\ell} \rangle$, the extracted values of m_t can be quite different according to whether one uses HERWIG or PYTHIA. In fact, as Tables 2 and 3 tell us that the typical difference between HERWIG and PYTHIA is $\langle m_{B\ell} \rangle \simeq 800 - 900 \text{ MeV}$, the corresponding uncertainty inferred on m_t can be up to about $\Delta m_t \simeq 2 \text{ GeV}$, given the slopes of the straight lines in Fig. 10. Such a value of Δm_t is clearly quite large, and much above the 600 MeV quoted in [10], thus

⁶We remind that, since we plotted $(1/\sigma)(d\sigma/dm_{B\ell})$ everywhere, our distributions are normalized to unity.

⁷Of course, given the numbers in Tables 2 and 3, a linear fit will work even for the higher Mellin moments of the $m_{B\ell}$ spectrum.

showing that probably such an error, obtained varying the ϵ parameter in the Peterson hadronization model, may have been underestimated. Our Δm_t is instead closer to the 2.1 GeV determined in [2] as the Monte Carlo systematic error when measuring m_t from the $m_{\mu\ell}$ spectrum at CDF.

Our analysis, however, assumes that one is indeed able to measure the full $m_{B\ell}$ spectrum, which is obviously quite ideal. A more realistic estimate of Δm_t due to the b -quark hadronization can be obtained if we discard the low- and high- $m_{B\ell}$ tails and restrict ourselves, e.g., to the range $30 \text{ GeV} < m_{B\ell} < 90 \text{ GeV}$. In this range, we obtain the truncated moments of the $m_{B\ell}$ spectrum presented in Tables 4 and 5. The discrepancy between HERWIG and PYTHIA is clearly smaller after we cut the tails of the spectrum; the linear relation of the moments with respect to m_t is nonetheless still preserved.

m_t (GeV)	$\langle m_{B\ell} \rangle$ (GeV)	$\langle m_{B\ell}^2 \rangle$ (GeV ²)	$\langle m_{B\ell}^3 \rangle$ (GeV ³)	$\langle m_{B\ell}^4 \rangle$ (GeV ⁴)
171	59.28	3.76×10^3	2.52×10^5	1.76×10^8
173	59.76	3.82×10^3	2.58×10^5	1.82×10^8
175	60.14	3.87×10^3	2.63×10^5	1.86×10^8
177	60.53	3.92×10^3	2.67×10^5	1.90×10^8
179	60.87	3.96×10^3	2.72×10^5	1.94×10^8

Table 4: Truncated moments of the $m_{B\ell}$ spectrum, according to HERWIG in the range $30 \text{ GeV} < m_{B\ell} < 90 \text{ GeV}$.

m_t (GeV)	$\langle m_{B\ell} \rangle$ (GeV)	$\langle m_{B\ell}^2 \rangle$ (GeV ²)	$\langle m_{B\ell}^3 \rangle$ (GeV ³)	$\langle m_{B\ell}^4 \rangle$ (GeV ⁴)
171	59.05	3.73×10^3	2.50×10^5	1.75×10^8
173	59.44	3.78×10^3	2.55×10^5	1.79×10^8
175	59.84	3.83×10^3	2.60×10^5	1.84×10^8
177	60.17	3.88×10^3	2.64×10^5	1.88×10^8
179	60.56	3.92×10^3	2.69×10^5	1.92×10^8

Table 5: As in Table 4, but using the PYTHIA event generator.

As done when considering the full $m_{B\ell}$ range, we try to express the average value

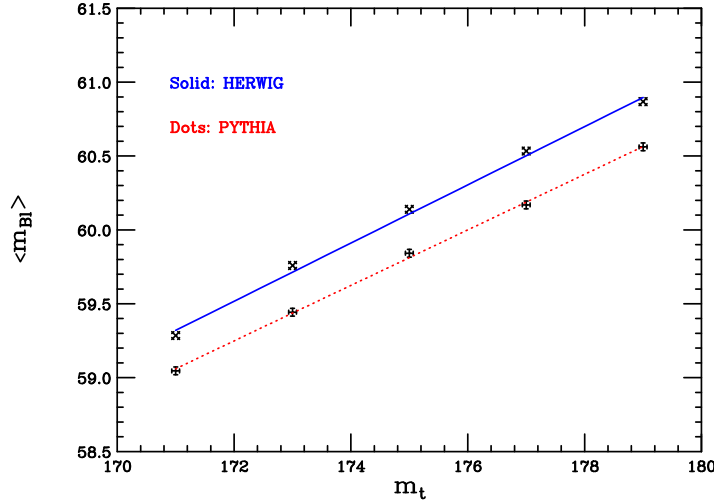


Figure 11: Linear fits of $\langle m_{B\ell} \rangle$, as a function of m_t , using HERWIG and PYTHIA in the range $30 \text{ GeV} < m_{B\ell} < 90 \text{ GeV}$.

$\langle m_{B\ell} \rangle$ in terms of m_t , according to a straight line. The best linear fits read:

$$\langle m_{B\ell} \rangle \simeq 25.63 \text{ GeV} + 0.20 m_t ; \quad \delta = 0.043 \text{ GeV} \quad (\text{HERWIG}) ; \quad (7)$$

$$\langle m_{B\ell} \rangle \simeq 26.93 \text{ GeV} + 0.19 m_t ; \quad \delta = 0.022 \text{ GeV} \quad (\text{PYTHIA}) . \quad (8)$$

The corresponding straight lines are plotted in Fig. 11. Since the found discrepancy between HERWIG and PYTHIA is about $\Delta \langle m_{B\ell} \rangle \simeq 250 - 300 \text{ MeV}$, and given the slopes of the straight lines in Fig. 11, the induced uncertainty on the top mass, thinking of extracting it by fitting the mean value $\langle m_{B\ell} \rangle$, goes down to $\Delta m_t \simeq 1.5 \text{ GeV}$. It is nonetheless still a quite large value, well above the estimate of the bottom-fragmentation contribution to the Monte Carlo error given in [10].

5 Conclusions

We performed a phenomenological study of bottom quark fragmentation in top-quark decay, using HERWIG and PYTHIA, the two most popular general-purpose Monte Carlo event generators. We observed that the default parametrizations are unable to reproduce B -hadron production data from ALEPH, OPAL and SLD, and therefore we used an ‘unofficial’ fit of the hadronization cluster and string models, following [11], in such a way to improve the description of such data.

We used this tuning to make predictions for a few observables in $t\bar{t}$ events, depending on modelling b -fragmentation in top decay, and found that the fits to e^+e^- data have a

remarkable impact even on top-decay observables. Moreover, HERWIG and PYTHIA results still exhibit visible discrepancies, which depend on the different quality of the fits to LEP and SLD data. We studied the B -energy fraction in top decay, which turned out to be roughly independent of the top mass, the B -lepton invariant mass $m_{B\ell}$, exhibiting relevant dependence on m_t , and the B transverse momentum in the laboratory frame, which can still be useful to determine the experimental acceptance for $t\bar{t}$ events, although it is not Lorentz-invariant and depends on the top-production mechanism as well.

Among these quantities, we have taken particular care about $m_{B\ell}$, whose spectrum is also interesting for the purpose of the analyses [2,10], where the top mass is reconstructed by using final states with leptons and J/ψ or muons.. We calculated the Mellin moments of the $m_{B\ell}$ distribution and parametrized the average value $\langle m_{B\ell} \rangle$ as a linear fit of the top mass. The found discrepancies between HERWIG and PYTHIA result in an uncertainty on the top mass, assuming that one can extract it from a fit of $\langle m_{B\ell} \rangle$, which can be up to $\Delta m_t \simeq 2$ GeV. The Monte Carlo error due to modelling b -fragmentation decreases down to $\Delta m_t \simeq 1.5$ GeV, if we restrict our analysis to the region around the invariant-mass peak, namely $30 \text{ GeV} < m_{B\ell} < 90 \text{ GeV}$. As such estimates are quite large, our study confirms that bottom fragmentation will play a crucial role in top-quark analyses at Tevatron and LHC and that having event generators reliably describing the $b \rightarrow B$ transition will be fundamental.

A possible extension of our work clearly consists in employing the object-oriented versions of HERWIG and PYTHIA, written in C++. In fact, the discrepancies here emphasized mainly depend on the fact that, even after the fits, fortran HERWIG is only marginally consistent with B -hadron data from LEP and SLD. Therefore, since the preliminary results presented in [18], obtained by comparing an early version of HERWIG++ with the SLD B -data, look encouraging, we believe that a lower Δm_t can eventually be obtained when using the C++ programs. However, the analysis carried out throughout this paper will still be valid as long as one uses MC@NLO or matrix-element generators interfaced to fortran HERWIG and PYTHIA for showers and hadronization.

We also stressed the fact that the fits carried out in Ref. [11] and reviewed in Section 2 just account for B -hadron data and may spoil the comparison with other observables, e.g., light-hadron data. In perspective, the advanced fitting code Professor [33] should be a very useful tool, as it is capable of improving the description of the x_B spectrum, but without spoiling too much possible agreement with other data. The use of the Professor program is currently in progress.

Furthermore, let us point out that, whereas in our study we aimed at predicting a few top-decay observables taking non-perturbative information from e^+e^- annihilation, possible hadron-collider data, for example on the $m_{B\ell}$ distribution, should be very useful to validate tools such as HERWIG or PYTHIA. This way, one could directly fit such spectra and tune the parameters of cluster and string models, without necessarily relying

on the fits to e^+e^- data. For the time being, we still believe that it can be nevertheless very interesting reconsidering the studies [2, 10], as they strongly rely on the Monte Carlo treatment of bottom fragmentation in top decay, and understand whether the results on Δm_t quoted in [2, 10] should change if one used the tuned versions of cluster and string models, as we did throughout this paper.

Acknowledgements

We acknowledge discussions with L. Cerrito, S. Leone, M.L. Mangano, M.H. Seymour, R. Tenchini and T. Sjostrand on these and related topics. The work of F.M. has been supported in part by CUR Generalitat de Catalunya under project 2009SGR502 and by the Consolider-Ingenio 2010 Program CPAN (CSD2007-00042).

References

- [1] A. Abulencia et al., CDF Collaboration, Phys. Rev. D 75 (2007) 071102(R);
T. Aaltonen et al., CDF Collaboration, Phys. Rev. D 79 (2009) 072001.
- [2] T. Aaltonen et al., CDF Collaboration, arXiv:0906.5371 [hep-ex].
- [3] V.M. Abazov et al., D0 Collaboration, Phys. Rev. D 74 (2006) 092005.
- [4] G. Corcella et al., JHEP 0101 (2001) 010.
- [5] T. Sjöstrand, S. Mrenna and P. Skands, JHEP 0605 (2006) 036.
- [6] B.R. Webber, Nucl. Phys. B 238 (1984) 492.
- [7] B. Andersson, G. Gustafson, G. Ingelman, T. Sjöstrand, Phys. Rept. 97 (1983) 31.
- [8] M.G. Bowler, Z. Phys. C 11 (1981) 169.
- [9] C. Peterson, D. Schlatter, I. Schmitt and P.M. Zerwas, Phys. Rev. D 27 (1983) 105.
- [10] A. Kharchilava, Phys. Lett. B 476 (2000) 73.
- [11] G. Corcella and V. Drollinger, Nucl. Phys. B 730 (2005) 82.
- [12] A. Heister et al., ALEPH Collaboration, Phys. Lett. B 512 (2001) 30.
- [13] G. Abbiendi et al., OPAL Collaboration, Eur. Phys. J. C 29 (2003) 463.

- [14] K. Abe et al., SLD Collaboration, Phys. Rev. Lett. 84 (2000) 4300.
- [15] G. Marchesini and B.R. Webber, Nucl. Phys. B 238 (1984) 1; ibid. B 310 (1988) 461.
- [16] T. Sjöstrand and P. Skands, Eur. Phys. J. C 39 (2005) 129.
- [17] M. Bahr et al, arXiv:0804.3053 [hep-ph];
- [18] S. Gieseke, P. Stephens and B.R. Webber, JHEP 0312 (2003) 045.
- [19] T. Sjöstrand, S. Mrenna and P. Skands, Comput. Phys. Commun. 178 (2008) 252.
- [20] S. Frixione and B.R. Webber, JHEP 0206 (2002) 029.
- [21] M.L. Mangano, M. Moretti, F. Piccinini, R. Pittau and A. Polosa, JHEP 0307 (2003) 001.
- [22] J. Alwall, P. Demin, S. de Visscher, R. Frederix, M. Herquet, F. Maltoni, T. Plehn, D.L. Rainwater and T. Stelzer, JHEP 0709 (2007) 028.
- [23] M. Cacciari and S. Catani, Nucl. Phys. B 617 (2001) 253.
- [24] G. Corcella and A.D. Mitov, Nucl. Phys. B 623 (2001) 247;
M. Cacciari, G. Corcella and A.D. Mitov, JHEP 0212 (2002) 015.
- [25] G. Corcella, Nucl. Phys B 730 (2005) 82.
- [26] B. Mele and P. Nason, Nucl. Phys. B 361 (1991) 626.
- [27] V.G. Kartvelishvili, A.K. Likhoded and V.A. Petrov, Phys. Lett. B 78 (1978) 615.
- [28] Yu.L. Dokshitzer, V.A. Khoze and L.H. Orr, Nucl. Phys. B 403 (1993) 65.
- [29] G. Corcella, J. Phys. G 26 (2000) 634.
- [30] G. Corcella, M.L. Mangano and M.H. Seymour, JHEP 0007 (2000) 004.
- [31] G. Corcella and M.H. Seymour, Phys. Lett. B 442 (1998) 417.
- [32] S. Leone, private communication.
- [33] P. Abreu et al., DELPHI Collaboration, Z. Phys. C 73 (1996) 11;
<http://projects.hepforge.org/professor/>